

LA-UR-79-533

MASTER

CONF. 790507--1

TITLE: EXPERIMENTAL SURVEY OF THE POTENTIAL ENERGY SURFACES ASSOCIATED WITH FISSION

AUTHOR(S): H. C. Britt

SUBMITTED TO: IAEA Symposium on Physics and Chemistry of Fission, Julich, West Germany, May 14-18, 1979

NOTICE
This report was prepared as an account of work sponsored by the United States Government. Neither the United States nor the United States Department of Energy, nor any of their employees, nor any of the contractors, subcontractors, or their employees, makes any warranty, express or implied, or assumes any liability or responsibility for the accuracy, completeness, or usefulness of any information, apparatus, product, or process disclosed, or represents that its use would not infringe privately owned rights.

University of California

By acceptance of this article, the publisher recognizes that the U.S. Government retains a nonexclusive, royalty-free license to publish or reproduce the published form of this contribution, or to allow others to do so, for U.S. Government purposes.

The Los Alamos Scientific Laboratory requests that the publisher identify this article as work performed under the auspices of the U.S. Department of Energy.



LOS ALAMOS SCIENTIFIC LABORATORY

Post Office Box 1663 Los Alamos, New Mexico 87545

An Affirmative Action/Equal Opportunity Employer



EXPERIMENTAL SURVEY OF THE POTENTIAL
ENERGY SURFACES ASSOCIATED WITH FISSION*

H. C. Britt

Los Alamos Scientific Laboratory, University of California
Los Alamos, New Mexico, USA

ABSTRACT

Progress in the experimental determination of the properties of the potential energy surface associated with fission is reviewed. The importance of nuclear symmetry effects on the calculation of fission widths is demonstrated. Evidence is presented for the fragmentation of the mass asymmetric second barrier in the thorium region and the axial asymmetric first barrier in the californium region. Detailed analyses of experimental data suggest the presence of two parallel second barriers; the normal mass asymmetric, axial symmetric barrier and a slightly higher mass symmetric, axial asymmetric barrier. Experimental barrier parameters are determined systematically and compared to calculations from various theoretical models. Techniques for expanding fission probability measurements to higher energies are discussed.

1. INTRODUCTION

The IAEA symposia on the physics and chemistry of fission have served both as periodic reviews of fission research and as a source for creating new perspectives and insights to influence further research. In these symposia a major topic has always been the experimental and theoretical attempts to define the characteristics of the potential energy surfaces that control fission decay rates. Progress in this field has generally been marked by occasional giant leaps in the qualitative nature of the theories followed by increasingly detailed experimental investigations. As in many fields the experiments tended to support the current theoretical concepts but at the same time they gradually contributed evidence that the theories were incomplete. In particular, the evolution in our understanding of fission has been steadily in the direction of demonstrating increasing complexity in the potential energy surfaces.

Shortly after the discovery of fission Bohr and Wheeler [1] showed that the fission barrier obtained from a liquid drop nuclear model when coupled with the concept of a fission width controlled by transition states at the barrier could explain the general properties of the

* Work supported by the US Department of Energy.

fission process as then known. This simple liquid drop model was used as the foundation for the interpretation of fission thresholds and decay rates for almost twenty-five years. However, at the first IAEA fission symposium there were just beginning to be signs of experimental phenomena that could not be understood in terms of the current theories. The most dramatic of the new observations were the discovery of fission isomers in americium isotopes [2]. The existence of fissioning isomers with excitation energies of 2-3 MeV and millisecond half lives was qualitatively inconsistent with the then current theories of fission. In addition, later experiments showed subbarrier resonances in fission probability distributions [3] and the existence of intermediate structure in low energy (n,f) resonance studies for some actinide nuclei 4,5. These results all pointed to inadequacies in the simple liquid drop theory of fission.

The key to the understanding of these puzzling phenomena came when Strutinski and collaborators in Copenhagen 6 and Nilsson and his group [7] in Lund followed up on an idea originally proposed by Swiatecki [8] that nuclear shells may have important effects in deformed as well as spherical nuclei. Using the method developed by Strutinski for applying shell corrections to a liquid drop potential energy surface it was shown that in the actinide region fission barriers should be double peaked with a well developed second minimum. This result gave a natural explanation for the experimentally observed isomeric phenomena and the 1969 IAEA conference was dominated by reports of theoretical calculations exploiting this new technique and experiments which showed that isomers and resonant structures were a common feature throughout the actinide region [9]. At this point the theory had jumped considerably ahead of the current experiments and it appeared that a quantitative understanding of the fission decay process in terms of basic physical concepts was at hand.

The period between the 1969 and 1973 IAEA fission conferences was one of intense activity by experimental and theoretical groups throughout the world. The theorists discovered the importance of triaxial and mass asymmetric degrees of freedom in their calculations [10-13] and the experimental groups developed methods for estimating fission barrier parameters from the growing volume of experimental results [14-16]. The 1973 conference included the first broad comparisons between theory and experiments [17-19]. It was found that good agreement was obtained in the middle of the actinide region (i.e. uranium and plutonium) but there were quantitative discrepancies between theory and experiment in the light actinides (thorium) and hints of problems in the heavy actinides (curium). Furthermore, there seemed to be a puzzling problem in the normalizations of the supposedly realistic microscopic statistical models that were used to analyse the experimental fission probability results [17].

In this review we will attempt to cover the major experimental results in this area since the last symposium in 1973. The major conceptual breakthrough came as a result of the observation by Bjornholm, Bohr, and Mottelson [20] that nuclear shape symmetries have fundamental effects on the magnitudes of the nuclear level densities. Incorporation of these symmetry effects into the current microscopic statistical models led to a model that could quantitatively reproduce the absolute magnitude of measured fission probabilities [21]. Armed with more realistic models and a continually expanding base of experimental data we are rapidly

discovering that the potential energy surfaces associated with fission must be much more complex than previously believed [22-25]. In particular, we may be discovering a new set of smaller shell corrections which produce 1-2 MeV fluctuations in the potential energy surface.

In the remainder of this paper we will present a discussion of the importance of nuclear symmetry effects for understanding fission probability distributions (Section 2); evidence for increased complexity of the potential energy surfaces associated with fission (Section 3); a re-analysis of existing experimental data in terms of our current concepts with a comparison to various theoretical predictions (Section 4) and a sample of some new experimental techniques that may be useful in expanding the measurements of Γ_f/Γ_n to higher excitation energy regions (Section 5). We will present and draw conclusions from current experimental data but the reader is referred to the original papers for discussions of the experimental techniques.

2. EXPERIMENTAL DETERMINATION OF FISSION BARRIER PARAMETERS

2.1. General Considerations

One of the major reasons for pursuing experimental programs to measure fission probability distributions and fission isomer excitation functions is to try to deduce the gross properties of the potential energy surface associated with fission. These "experimental" fission barrier parameters can then be compared with various theoretical calculations.

Figure 1 illustrates schematically the two types of experiment that have been used to obtain most of the current information on fission barrier heights [5]. In a direct reaction fission experiment a direct reaction (or neutron absorption reaction) is used to excite a residual nucleus to a particular excitation energy and the branching ratio for decay by fission relative to neutron or gamma ray deexcitation (or the fission cross section) is measured. This type of experiment [17,18,26,27] gives information on the height and curvature of the highest peak in the fission barrier. In addition, for cases where $E_A \approx E_B$ or where fission transmission resonances are observed estimates can be obtained for the parameters of both barriers. In the case of fission isomer experiments the results depend most sensitively on E_B and E_{II} [14]. Since most isomers occur for heavy actinides (Pu, Am, Cm) where $E_A \approx E_B$, the direct reaction and isomer experiments tend to be complementary. During the last several years data have been obtained on fission probability distributions for most of the actinide nuclei which can be reached using available target isotopes and a wide variety of direct and neutron capture reactions. In addition, excitation functions for most of the accessible fission isomers have been measured. Thus, we now have an almost complete set of experimental data for use in systematizing the gross properties of fission barriers throughout the actinide region.

During the last several years considerable progress has also been made in the development of microscopic statistical models which could be used to extract barrier parameter estimates from fits to experimental data. The major inputs to these models for the analysis of nonresonant data are the level densities as a function of excitation energy at the

saddle points and minima of the potential energy surface. These level densities are used for the estimate of the relevant decay widths, Γ_f , Γ_n , and Γ_γ . A major advance in the development of more realistic models was the incorporation of microscopic level densities which could be obtained directly from the relevant single particle spectra that were used to calculate the potential energy surfaces [14,27]. This approach gives more realistic estimates for the slope of the level density function in the critical energy region of 0-5 MeV and eliminates the need for arbitrary parameters that were necessary in previous statistical models.

When resonance structures are observed in the experimental data more detailed information on the potential energy surface can be extracted. In these cases experimental data have been most commonly analysed using models which incorporate resonances generated by the penetrability through a one-dimensional double-peaked fission barrier that has been parameterized by a smooth joining of three parabolic sections [28]. Models of this type are qualitatively successful in reproducing the experimental results. However, there is increasing evidence for the importance of deviations in barrier shapes from simple parabolas, and the variation of the barrier shapes with spin, parity and K value. Also, as we begin to accumulate evidence for increased complexity in the potential energy surfaces the adequacy of a simple one-dimensional approach for the quantitative analysis of resonance phenomena becomes more doubtful. Some of these points will be discussed in more detail in subsequent sections.

2.2 Nuclear Symmetry Effects on Level Densities

In the calculations of fission probabilities, P_f , the important quantities are branching ratios between fission, neutron emission and gamma de-excitation and these ratios generally involve ratios of level densities and not their absolute magnitudes. In the first attempt to use microscopic level densities for P_f calculations, a single normalization factor (determined from comparison to measured level spacing at the neutron binding energy) and an empirical spin distribution were used to generate level densities from the calculated microscopic state densities [27]. It was felt that any errors in this simplified approach would tend to cancel out in the ratios that come into the P_f calculations. When this model was applied to the analysis of fission probability data it was found that the shapes of the distributions near threshold could be reproduced but an arbitrary normalization of Γ_f/Γ_n was necessary to reproduce the absolute magnitudes of the measured P_f values. Furthermore, this normalization factor varied from a value of ≈ 1 for thorium isotopes to a value of ≈ 0.1 for heavy actinides. A more serious difficulty with this model became apparent when comparisons were made to new data taken to higher excitation energies using ($^3\text{He},df$) and ($^3\text{He},tf$) reactions. It was found that the microscopic statistical model could not in many cases reproduce the shapes of the measured P_f distributions in the excitation energy region from threshold to ≈ 5 MeV above threshold. In particular the model when normalized in the threshold region would tend to seriously underestimate P_f at higher excitation energies.

The clue toward understanding the major deficiency of this model came from a paper at the 1973 conference where Bjornholm, Bohr and Mottelson [20] pointed out that at low energies nuclear symmetry effects have a very important influence on the level densities for deformed systems. In

particular they showed the necessity of combining low lying rotational excitations with the single particle state densities obtained from microscopic calculations. Since the density of these rotational excitations depends on the degree of symmetry in the nuclear system, this approach leads to a dependence of the nuclear level density on the symmetry of the nucleus at the relevant minimum and saddle points in the potential energy surface. This effect is not important when considering the ratio of neutron to gamma ray decay where both decays occur from the nucleus in the same configuration (i.e. in the first potential minimum). However, there is a large effect when comparing the decay of neutrons or gamma rays from the axially and mass symmetric first minimum to fission which involves the passage over two saddle points the first with a triaxial shape and the second with a mass asymmetric, axial, symmetric shape [21].

Figure 2 shows examples of microscopic state densities at the three points in the potential energy surface that are important in determining P_f . In addition, the level density at the first saddle point is shown for various assumptions about the symmetry of the nuclear shape. The results show that the state density, $\omega(E^*)$, is very similar at the first minimum, the axially asymmetric first saddle and the mass asymmetric second saddle. The similarity in $\omega(E^*)$ is partly due to the similar shell corrections at all three points but is also due to the fact that at low energies the shell and pairing corrections tend to have opposite effects on $\omega(E^*)$ and lead to a function which is relatively insensitive to the single particle spectrum used to generate the state density. In contrast, there is a large dependence of the nuclear level density, $\rho(E^*)$, on the nuclear symmetry. The large change comes about from a breaking of the m-state degeneracy when a spherical nucleus is deformed and the coupling to low lying rotational excitations. The level density for a system with no symmetries (i.e. triaxial with no point group symmetries) is enhanced over an axially symmetric prolate deformation due to the increased number of independent rotational excitations that become possible.

The effect of these level density enhancements on the calculated fission probabilities is shown in Fig. 3 for a model fit to P_f data for ^{239}Np . If it is assumed that the first saddle has an axially asymmetric shape a good fit can be obtained. Using the same barrier parameters but assuming an axially symmetric shape at the first saddle leads to a significant reduction in the calculated P_f and change in shape so that even if the calculations are renormalized the data can not be fit in both the barrier and 8-10 MeV excitation energy regions. The reason for the change in shape of the calculated P_f distributions is illustrated in Fig. 4. In the case where E_A is greater than E_B by a small amount (0.4 MeV in this case) if symmetry effects are neglected the fission probability is always determined by the level density at the first saddle (i.e. N_A is always less than N_B). However, for an axially asymmetric first barrier N_A increases more rapidly than N_B so that near threshold P_f depends most sensitively on E_A while at higher energies E_B is the most important parameter. Assuming an axially asymmetric first barrier made it possible to obtain qualitatively good fits to fission probability data throughout the actinide region for excitation energies up to ≈ 12 MeV without introducing any arbitrary normalization parameters. Typical fits for a series of Np isotopes are shown in Fig. 5. These results provide indirect but compelling evidence that the first

is in fact axially asymmetric for most of the actinide region as was predicted by theoretical calculations of the potential energy surface [2,13].

3. EVIDENCE FOR INCREASED COMPLEXITY IN THE POTENTIAL ENERGY SURFACE

3.1. The Ra-Th Anomaly

At the 1973 Fission Conference detailed comparisons of fission barrier parameters from fits to experimental data were compared to results from various theoretical calculations of the potential energy surfaces [17-19]. These comparisons showed qualitative agreement in the U-Pu region but there seemed to be a serious disagreement for some thorium isotopes. In particular most theoretical calculations [19,29-31] indicated that the first saddle should be 2-3 MeV lower than the second saddle and, thus, the observed fission probability distributions should be smooth and structureless reflecting the smooth dependence for the penetrability through a single peaked fission barrier. In contrast Fig. 6 shows P_f distributions for ^{231}Th and ^{234}Th where very dramatic resonance phenomena are observed. These results indicate the peaks of the two barriers are of approximately equal height and the very sharp resonance in ^{231}Th indicates much less damping than is present in heavier actinide nuclei where only the even-even nuclei show resonance structures. A detailed analysis of the ^{231}Th data [32] indicated the potential minimum between the two barriers had a depth of less than 2 MeV as compared to \approx 3-4 MeV for Pu and Am isotopes.

A possible explanation for the apparent qualitative difference between experimental results and theoretical calculations was suggested by Moller and Nix at the 1973 Conference [19] and shown to be qualitatively reasonable in a later publication [31]. They suggested that the two peaks responsible for the observed resonance phenomena might be due to the development of a third potential minimum in the region of the second mass-asymmetric saddle point. If this explanation were correct it would represent the first case in which secondary shell fluctuations (1-2 MeV) have been observed in the potential energy surface. The region of the second saddle for thorium isotopes is the most likely place to observe those smaller shell structures because a very broad second barrier is produced by the overlap of the peak of the liquid drop saddle with the major antishell that creates the second barrier in actinide nuclei.

Since 1973 two different experimental investigations have led further credence to the postulate of a third potential minimum for light actinides. Figure 7 shows the fission probability obtained for ^{228}Ra [23]. In this case it was shown that the sharp structure at \approx 8 MeV could only be reproduced by assuming a resonant penetration of two barriers at \approx 8 MeV separated by a shallow minimum. Theoretical calculations [29] predicted $E_A \approx$ 4.2 MeV and $E_B \approx$ 8.7 MeV so that the most reasonable interpretation of the resonance phenomena was in terms of the postulated third minimum. Finally, very recent high resolution experiments on the ^{231}Th resonance [33] have indicated complex fine structure which can be most simply interpreted in terms of a level structure in the third minimum that consists of two overlapping $K = 1/2$ rotational bands with the opposite parity and essentially no mixing or damping into underlying compound states. The moment of inertia and decoupling parameter these two bands are found to be the same and are

consistent with the deformations expected for the second saddle point rather than the normal second minimum. Since two identical almost degenerate bands of opposite parity are a signature for a mass asymmetric shape these results would seem to give the final experimental confirmation of the third minimum postulate.

3.2. Barriers for nuclei with $N = 150-156$

Another region where fission thresholds show an unexpected behavior is near the $N = 152$ shell [22,25]. It has long been known that ground state masses indicate an apparent shell closure for $N = 152$ [34] and that there is a sharp discontinuity in the trend of spontaneous fission half lives at this neutron number [35]. The presence of shell effects in this region are also indicated by fission probability measurements (Fig. 8) where it has been shown that for both curium and californium isotopes there is a drop in the fission threshold when the neutron number is increased from $N = 152$ to $N = 154$. Additional measurements [36] on einsteinium nuclei (Fig. 9) with $N = 156$ and $N = 157$ indicate values for E_A of 5.4 MeV and 4.8 MeV, respectively, which are rather similar to ^{250}Cm and ^{252}Cf . These results taken together suggest a significant decrease in E_A for $N > 152$. Furthermore, in the case of ^{250}Cm a weak resonance at 4 MeV established the height of the second barrier at 4.4 MeV [37] in qualitative agreement with fission isomer results for lighter curium isotopes and with theoretical predictions.

The most surprising aspect of these data is the appearance of resonance like structures in ^{252}Cf at excitation energies in the region 5-5.5 MeV and the hint of similar structure in ^{255}Es . These resonances are broader and occur with much larger fission probabilities than any of the transmission resonances observed for lighter actinides. Such a structure could occur from a double peaked fission barrier if the two peaks were very sharp. The appearance of resonant structure for both even-even and odd mass nuclei suggest a shallow minimum as in the case of thorium isotopes. Furthermore, the two apparent resonances in ^{252}Cf have quite different anisotropies suggesting that there may be closely spaced resonances with different K values. Closely spaced resonances in an even-even system with different K values have not been previously observed and are consistent with the presence of an axially asymmetric system which would be expected to show approximately degenerate rotational bands with $K = 0$ and $K = 2$.

In analogy to the thorium results these data appear consistent with the postulate that in this region secondary shell effects have caused the first axially asymmetric saddle point to break into two sharp barriers or at least to become lumpy enough that it deviates significantly from a parabolic shape. A fragmentation of the first barrier would most likely occur in this region since the liquid drop saddle has approximately the same deformation as the first strong antishell. Thus, this is a region where conditions for the first barrier are very similar to those encountered in thorium for the second barrier. The conclusions can not be made as strongly as for thorium but in one respect the situation is somewhat clearer. In this case it seems clear that we are not seeing transmission resonances through the same two barriers as for lighter actinides because for ^{250}Cm a resonance that can be associated with the "normal" second barrier is observed at a much lower energy. Thus, these results again point to the presence of secondary shell structure on the potential

energy surface which can be observed under the appropriate experimental conditions.

3.3. The Symmetric Second Saddle Point

For many years there has been considerable interest in the fission of radium and actinium isotopes. In this region fission mass distributions show distinctly separable symmetric and asymmetric components [38], the excitation functions for these components are quite different, and they seem to indicate different thresholds for the two mass components [39]. Attempts have been made to try to correlate this behavior with characteristics of the second saddle point in the potential energy surface [40, 41]. These attempts were, in general, not very convincing because the theoretical calculations of the potential energy surface as a function of mass asymmetry did not show evidence for a separate saddle point at symmetry.

Figure 10 shows excitation functions for symmetric and asymmetric mass components [39] for a series of actinium nuclei. The results indicate a threshold for the symmetric component that is 1-2 MeV higher than for the asymmetric component [39]. Similar results have been obtained for ^{228}Ra [23] and Fig. 11 shows the excitation functions for the symmetric component along with the results obtained from attempts to fit the data with the microscopic statistical model described in Section 2. The solid line represents the best fit that can be obtained if it is assumed that the fission barrier is axially symmetric and mass asymmetric. It is seen that the model is unable to reproduce the rather slowly rising fission probability that is observed both for this case and for the previous actinium data [39]. However, if we arbitrarily assume that symmetric fission involves a separate barrier that is axially asymmetric then the dashed curve is obtained which gives a much better characterization of the experimental data.

At about the same time as the attempt to analyse the ^{228}Ra data, results became available on the fission probability for ^{238}U in the excitation energy region 6 - 12 MeV from studies with monoenergetic photons [42]. ^{238}U is a particularly interesting case because previous data from (t, pf) [26] and (γ, f) [43] studies near threshold could be used to establish the parameters of the fission barrier for both positive and negative parity transition state bands. The results of these fits [24] are shown in Fig. 12 and the dashed curve in the top portion shows the extrapolation of the fit to higher energies. It is seen that the model calculations underestimate P_f by about a factor of 4 at excitation energies above 10 MeV. In analogy to our conclusions for ^{228}Ra we decided to investigate the result of adding another parallel second barrier which was axially asymmetric so that at higher excitation energies it would provide an enhanced fission probability. The solid curve in Fig. 12 shows that adding a parallel second barrier which is 0.3 MeV above the "normal" mass asymmetric barrier yields a good fit for the higher energy P_f measurement.

In order to test the credibility of this postulate of two parallel second barriers detailed potential energy calculations were done in the mass asymmetry-axial asymmetry plane in the region of the second saddle. The results are shown in Fig. 13. These results show two distinct saddle

points separated by ≈ 1 MeV for ^{228}Ra in agreement with the conclusions from the model fits. For ^{238}U there is also evidence for two saddles with a separation of ≈ 0.5 MeV. In the ^{238}U case the ridge between the two saddles is not as distinct as for ^{228}Ra .

Recent attempts to systematically refit the P_f data [37] for actinide nuclei have also shown that the inclusion of an axially asymmetric parallel second barrier which is ≈ 0.5 MeV above the normal mass asymmetric barrier either improves the quality of the fit or gives a more consistent set of values for the height of the mass asymmetric barriers. Taken together these results indicate both experimentally and theoretically the existence of two parallel second barriers one of which is mass asymmetric, axially symmetric and the other at an excitation energy about 0.5 MeV higher is mass symmetric and axially asymmetric.

It is interesting to note that while the two mass components for ^{228}Ra can be approximately identified with fission over the two parallel saddle points the same is not true for ^{238}U . For ^{238}U such a correlation would predict predominately symmetric fission at excitation energies above 10 MeV and this is not observed experimentally. For ^{238}U the lack of a sharp ridge between the two saddles probably means that the nucleus can travel over the mass symmetric saddle and later on the descent toward scission it can go over to a mass asymmetric configuration.

4. SYSTEMATICS OF FISSION BARRIER PARAMETERS

As has been shown in the preceding sections our perceptions of the general characteristics of the potential energy surfaces and the level density functions associated with the fission process have sharpened considerably over the past five years. In addition, the data base on fission probabilities for actinide nuclei has broadened and we are now at the point where data near threshold for most of the fissioning systems that can be conceivably investigated is available. Thus, this seems an appropriate time to attempt a reanalysis of all the available data in a consistent manner using our current version of a microscopic statistical model as described qualitatively in Section 2 and in previous papers [21,26,27].

The details of the model, fitting criteria, input data and the fits to various data sets will be described in a forthcoming comprehensive review [37]. In this section we will only describe some very general features and then compare the barrier parameters extracted from the experimental data with results obtained in other ways with the theoretical predictions of several groups.

In fitting the experimental data we have assumed that the first barrier has no symmetry except for the lightest actinides (Th, Pa) where reasonable fits could be obtained with the assumption of axial symmetry. For cases where the data extended to energies well above threshold we have assumed two parallel second barriers with a separation of 0.5 MeV. In general, we have tried to find a systematic set of parameters where E_A , E_B and the curvatures $h\omega_A$ and $h\omega_B$ vary smoothly. From a study of the fits and a comparison to previous analyses we believe that the systematic uncertainties in the determination of barrier parameters from experimental fission probabilities are of the order ≈ 0.3 MeV for

the higher of the two barriers or for both barriers when $E_A \approx E_B$. For a difference of 0.5 - 1.0 MeV between the two barriers the uncertainty on the lower one may be as large as ≈ 0.5 MeV and for a difference greater than 1 MeV the lower barrier can not be reliably determined except in cases where transmission resonances are observed.

The results from this systematic analysis of experimental data are shown in Fig. 14. In general, the dependence of E_A and E_B on neutron number for a particular element is relatively smooth. The occasional fluctuations with odd or even masses are relatively small and could be due to systematic uncertainties in the relative Γ_γ and Γ_n calculations since the fission thresholds systematically fluctuate from above to below the neutron binding energy as the neutron numbers change from odd to even. Also shown in Fig. 14 are values for E_B that have been previously obtained from the analysis of fission isomer excitation functions [44] and barrier parameters for Pu and Am isotopes deduced by the Bordeaux - Stony Brook collaboration [44-47] from systematic fits to fission probabilities, fission isomer excitation functions and excitation functions for xn reactions. The various results are all internally consistent to within an average of $\approx 0.2-0.3$ MeV which is consistent with our estimates of the reliability of current measurement and analysis techniques. In Fig. 14 we also show estimates for E_A and E_B that are obtained from an analysis [48] of the widths of sub-barrier fission resonances for a series of U, Np and Pu isotopes excited in (n,f) resonances. On the average these results are in good agreement with the results from excitation function analyses. Individual deviations are observed up to ≈ 0.5 MeV but some of this could be due to the different spin states excited in the direct reaction and low energy (n,f) experiments. In general the agreement for values of the barrier parameters extracted from fission probability data, xn isomer and ground state excitation functions and sub-barrier resonance widths indicate that most of the systematic errors have been eliminated in the current analyses. For the thorium and proto-actinium nuclei both barriers should probably be associated with the second saddle and they are plotted that way in the lower portion of the figure.

In Fig. 15 the experimental barrier parameters are compared to predictions from three theoretical calculations. The calculations by Moller [29] use a modified harmonic oscillator potential and the Lysekil liquid drop constants. The first barrier has been lowered to account for the effects of axial asymmetric deformations using the energy differences calculated by Larsson and Leander [49]. The calculations of Moller and Nix [31] use a droplet model for the underlying liquid drop surface and a folded Yukawa potential. In both of these calculations the potentials are fitted to obtain the best representation of known single particle levels for a variety of deformed actinide nuclei. The third set of calculations from Pauli and Ledergerber [30] are most similar to the folded Yukawa model except that in this case the authors: 1) adjusted the parameters of the liquid drop to obtain an approximate fit to fission barrier parameters rather than fixing them with a fit to ground state masses and 2) a Woods-Saxon potential was fitted to the known single particle spectrum of ^{208}Pb . For the last two calculations the effects of axial deformation at the first saddle were not systematically studied. In the results known in Fig. 15 the corrections of Larsson and

Leander [49] have been applied to the E_A values from both Moller and Nix, and Pauli and Ledergerber. The Moller and Nix uncorrected values of E_A are also shown to illustrate the magnitude of this correction.

From Fig. 15 it is seen that the calculations agree with each other and with the experimental barriers to an accuracy of $\approx 1-2$ MeV. The overall agreement appears best with the calculations of Moller but there are noticeable local and systematic deviations that could be a basis for further study. The results shown in Figs. 14 and 15 indicate that we have now evolved to a point where the experiments give a broad survey of barrier parameters with a systematic accuracy (≈ 0.3 MeV) that is considerably better than the theoretical predictions ($\approx 1-2$ MeV). There has been very little work done recently on refining the theoretical calculations and these results suggest that the experimental situation may now have evolved to a point where a new systematic theoretical study would be profitable. Because of the many differences in the theoretical models used in the calculations shown in Fig. 15 it is not possible to pinpoint whether current deficiencies lie primarily in the single particle shell corrections or in the underlying macroscopic liquid drop model. A comprehensive study of the macroscopic liquid drop part of this theory is planned in the near future to see if this might be a major cause of the systematic deviations between theory and experiment [50].

5. Γ_f/Γ_n MEASUREMENTS TO HIGHER ENERGIES

In the preceding sections we have seen that the experimental studies of fission probabilities for actinide nuclei in the excitation energy range from threshold to the onset of second chance fission (11-12 MeV) has been rather systematically and completely investigated. In this region we also understand in reasonable detail the interpretation of the data in terms of the properties of the underlying potential energy surface and microscopic level density functions.

In this section we will briefly describe some new feasibility studies aimed at investigating whether other types of direct reactions can be used to obtain fission probability data for excitation energies in the region of 10-20 MeV. From a detailed analysis of systematic data in this region it might be possible to obtain a more comprehensive view of several interesting aspects of the fission process. In the higher excitation energy regions it appears that a simple extrapolation of the model described in Section 2 gives too large a value of ρ . There are two general effects which should become important at higher excitation energies. First, the relative insensitivity of the microscopic state densities to the input single particle levels (see Fig. 2) tends to diminish and it may be possible from a systematic analysis to test various theoretical models in a new way. A second and more complex effect is that at higher energies the shell effects should start to wash out and cause a shift in the minimum of the level density functions away from the static saddle points [52] so that at a sufficiently high energy the deformation which gives the state density appropriate for an estimate of Γ_f would correspond to the liquid drop saddle. A related and possibly more complex effect is that as the level density minimum shifts toward the liquid drop saddle the symmetry enhancement effects will change.

Systematic data to higher excitation energies have been previously obtained for a series of neptunium isotopes from studies of (p,f) reactions on uranium isotopes [52]. One difficulty with this or with direct-reaction fission techniques is that at higher energies in many cases P_f tends to approach 1 so that the requirements for experimental accuracy in order to obtain useful information become very severe. In an attempt to try to get around this difficulty we have been studying a new technique that involves the detection of evaporation residuals following a direct reaction [53,54]. These are the actinide nuclei which survive fission and decay by xn evaporation. The measurement gives a probability $P_{ER} = 1 - P_f$ which has greater sensitivity for cases where P_f approaches 1. A recent experiment of this type [54] is illustrated in Fig. 16. Evaporation residuals are deflected out of plane to eliminate elastic ${}^7\text{Li}$ particles and a coincidence required with backward reaction alpha particles. The (${}^7\text{Li}, \alpha$) reaction leads primarily to residual excitations in the region 14-20 MeV. Thus, this technique seems to be a reasonable candidate for extending our detailed knowledge of Γ_f/Γ_n up to the next higher region of excitation energies.

Another reaction that has been recently studied [54] is the (${}^{12}\text{C}, {}^8\text{Be}$) reaction where the two alpha particles from the ${}^8\text{Be}$ breakup are detected in a semiconductor detector telescope. This reaction yields residual excitations in the 6-16 MeV region and, thus, is very good for studying the region of the onset of second chance fission. Results for the excitation of ${}^{236}\text{U}$ are shown in Fig. 17 and it is seen that the data are in good agreement with previous (t,pf) and (n,f) results

6. SUMMARY

This seems like a particularly good time to attempt a summary of our understanding of the potential energy surfaces that govern the fission process and in this review we have tried to accomplish this task. The data set on fission properties is qualitatively complete in the sense that we have information on fission probabilities and fission isomer properties for almost all nuclei that can be realistically investigated. These data have been analysed in a variety of models and yield a set of barrier parameters, E_A and E_B to an approximate accuracy of about 0.3 MeV. Thus, a reasonable data set exists for use in testing future theories. Comparisons to presently available theoretical calculations indicate a reliability of the order of 1-2 MeV.

Among the more interesting developments of the last few years has been the development of a very strong experimental case for the fragmentation of the second barrier in the Ra-Th region, evidence for more structures in the first barrier in the Cm-Cf region, and evidence that there are probably two parallel paths to fission in the region of the second barrier for most actinide nuclei. The parallel paths simply indicate that there is more than one way for the nucleus to avoid the large antishell region that occurs for axial and mass symmetric shapes. The increased structure in the potential energy surface is most probably just due to the influence of small second order shells which will tend to produce 1-2 MeV "wiggles" that are then superimposed on the "normal" two peaked fission barrier. We should expect that further more detailed experiments will shed more light on both of these effects.

Finally, the extension of fission probability measurements to higher energies is discussed. This represents another promising area for continuing experimental and theoretical research.

ACKNOWLEDGMENT

It is a pleasure to acknowledge useful discussion and critical comments from many colleagues and collaborators. In particular, B. B. Back, E. Cheifetz, J. R. Nix, H. Weigmann and J. B. Wilhelmy have contributed very substantially to the ideas and insights presented in this manuscript.

REFERENCES

- 1 N. BOHR and J. A. WHEELER, Phys. Rev. 56 (1939) 426.
- 2 S. M. POLIKANOV, V. A. DRUIN, V. A. KARNAUKOV, V. L. MIKHEEV, A. A. PLEVE, N. K. SKOBELEV, V. G. SUBBOTIN, G. M. TER-AKOP'JAN, and V. A. FOMICHEV, Zh. Eksp. Teor. Fiz. 42 (1962) 1464; G. N. FLEROV, A. A. PLEVE, S. M. POLIKANOV, E. IVANOV, N. MARTALOGU, D. POENARU and N. VILCOV, Physics and Chemistry of Fission (International Atomic Energy Agency, Vienna, 1965) 307.
- 3 H. C. BRITT, F. A. RICKEY, JR., AND W. S. HALL, Phys. Rev. 175 (1968) 1525.
- 4 E. MIGNECO AND J. P. THEOBALD, Nucl. Phys. A112 (1968) 603.
- 5 A. FUBINI, J. BLONS, A. MICHAUDON, and D. PAYA, Phys. Rev. Lett. 20 (1968) 1373.
- 6 V. M. STRUTINSKI, Nucl. Phys. A95 (1967) 420; A122 (1968) 1; M. BRACK, J. DAMGAARD, A. STEHOLM-JENSEN, H. C. PAULI, V. M. STRUTINSKI, and C. Y. WONG, Rev. Mod. Phys. 44 (1972) 320.
- 7 S. G. NILSSON, C. F. TSANG, A. SOBICZEWSKI, Z. SZYMANSKI, S. WYCFCH, C. GUSTAFSON, I. L. LAMM, P. MOLLER and B. NILSSON, Nucl. Phys. A131 (1969) 1.
- 8 W. J. SWIATECKI, Phys. Rev. 100 (1955) 937.
- 9 Second IAEA Symposium on Physics and Chemistry of Fission, (International Atomic Energy Agency, Vienna, 1969) Sections C, D, E.
- 10 P. MOLLER and S. G. NILSSON, Phys. Lett. 31B (1970) 283.
- 11 H. C. PAULI, T. LEDERGERBER and M. BRACK, Phys. Lett. 34B (1971) 264.
- 12 S. E. LARSSON, I. RAGNARSSON and S. G. NILSSON, Phys. Lett. 38B (1972) 269.
- 13 U. GOTZ, H. C. PAULI, and K. JUNKER, Phys. Lett. 39B, (1972) 436.
- 14 H. C. BRITT, M. BOLSTERLI, J. R. NIX and J. L. NORTON, Phys. Rev. C7 (1973) 801; H. C. BRITT, S. C. BURNETT, B. H. ERKKILA, J. E. LYNN and W. E. STEIN, Phys. Rev. C4 (1971) 1444.
- 15 J. E. LYNN, Second IAEA Symposium on Physics and Chemistry of Fission (International Atomic Energy Agency, Vienna, 1969) 249.
- 16 B. B. BACK, J. P. BONDORF, G. A. OTROSCHENKO, J. PEDERSEN and B. RASMUSSEN, Nucl. Phys. A165 (1971) 449.
- 17 B. B. BACK, OLE HANSEN, H. C. BRITT, J. D. GARRETT, and B. LEROUX; Physics and Chemistry of Fission, 1973 (IAEA, Vienna, 1974) I 3.
- 18 B. B. BACK, OLE HANSEN, H. C. BRITT, and J. D. GARRETT, *ibid* I 25.
- 19 P. MOLLER and J. R. NIX, *ibid* I 103
- 20 S. BJORNHOLM, A. BOHR, B. R. MOTTELSON, *ibid* I 367.

- 21 A. GAVRON, H. C. BRITT, E. KONECNY, J. WEBER, and J. B. WILHELMY, Phys. Rev. C13 (1976) 2374.
- 22 B. B. BACK, OLE HANSEN, H. C. BRITT, and J. D. GARRETT, Phys. Lett. 46B (1973) 183.
- 23 J. WEBER, H. C. BRITT, A. GAVRON, E. KONECNY, and J. B. WILHELMY, Phys. Rev. C13 (1976) 2413.
- 24 A. GAVRON, H. C. BRITT, P. D. GOLDSTONE, and J. B. WILHELMY, Phys. Rev. Lett, 38 (1977) 1457.
- 25 H. C. BRITT, A. GAVRON, P. D. GOLDSTONE, R. SCHOENMACKERS, J. WEBER, and J. B. WILHELMY, Phys. Rev. Lett. 15 (1978) 1010.
- 26 B. B. BACK, OLE HANSEN, H. C. BRITT, and J. D. GARRETT, Phys. Rev. C9 (1974).
- 27 B. B. BACK, H. C. BRITT, OLE HANSEN, B. LEROUX, and J. D. GARRETT, Phys. Rev. C10 (1974) 1948.
- 28 J. D. CRAMER and J. R. NIX, Phys. Rev. C2 (1970) 1048.
- 29 P. MOLLER, Nucl. Phys. A192 (1972) 529.
- 30 H. C. PAULI and T. LEDERGERBER, Nucl. Phys. A175 (1971) 545.
- 31 P. MOLLER and J. R. NIX, Nucl. Phys. A229 (1974) 269.
- 32 J. D. JAMES, J. E. LYNN, and L. EARWAKER, Nucl. Phys. A189 (1972) 225.
- 33 J. BLONS, C. MAZUR, D. PAYA, M. RIBRAG, and H. WEIGMANN, Phys. Rev. Lett. 41 (1978) 1282.
- 34 N. B. GOVE and A. H. WAPSTRA, Nucl. Data Tables 11 (1972) 127.
- 35 M. NURMIA, T. SIKKELAND, R. SILVA, and A. GHIORSO, Phys. Lett. 26B (1967) 78.
- 36 H. C. BRITT, E. CHEIFETZ, and J. B. WILHELMY, to be published.
- 37 H. C. BRITT and B. B. BACK, to be published.
- 38 H. C. BRITT, H. E. WEGNER, and J. C. GURSKY, Phys. Rev. 129 (1963) 2239.
- 39 E. KONECNY, H. J. SPECHT, and J. WEBER, Physics and Chemistry of Fission, 1973 (IAEA, Vienna, 1974) I 13.
- 40 C. F. TSANG and J. B. WILHELMY, Nucl. Phys. A184 (1972) 417.
- 41 A. S. JENSEN and T. DOSSING, Physics and Chemistry of Fission, 1973 (IAEA, Vienna, 1974) I 409.
- 42 J. T. CALDWELL, E. J. DOWDY, B. L. BERMAN, R. ALVAREZ, and P. MEYERS, Los Alamos Scientific Laboratory Report No. LAUR-76-1615.
- 43 P. A. DICKEY and P. AXEL, Phys. Rev. Lett. 35 (1975) 501.
- 44 J. GILAT, A. FLEURY, H. DELAGRANGE, and J. M. ALEXANDER, Phys. Rev. C16 (1977) 694.
- 45 H. DELAGRANGE, A. FLEURY, and J. M. ALEXANDER, Phys. Rev. C17, (1978) 1706.
- 46 A. FLEURY, H. DELAGRANGE, and J. M. ALEXANDER, Phys. Rev. C17 (1978) 1721.
- 47 J. P. GIREME, M. GRAFFEUIL, H. DELAGRANGE, and A. FLEURY, in preparation.
- 48 H. WEIGMANN, private communication.
- 49 S. E. LARSSON and G. LEANDER, Physics and Chemistry of Fission, 1973 (IAEA, Vienna, 1973) 177.
- 50 J. R. NIX, private communication.
- 51 V. S. RAMAMURTHY, S. S. KAPOOR, and S. K. KATARIA, Phys. Rev. Lett. 25 (1970) 386.
- 52 J. R. BOYCE, T. D. HAYWARD, R. BASS, H. W. NEWSON, E. G. BILPUCH, F. O. PURSER, and H. W. SCHMITT, Phys. Rev. C10 (1974) 231.
- 53 P. D. GOLDSTONE, H. C. BRITT, R. SCHOENMACKERS, and J. B. WILHELMY, Phys. Rev. Lett. 38 (1977) 1262.

FIGURE CAPTIONS

FIG.1. Systematic illustration of the major features of the direct reaction fission and fission isomer population processes.

FIG.2. Calculated nuclear state densities at the first minimum, first axially asymmetric saddle and second mass asymmetric saddle (lower portion). Calculated nuclear level densities at the first saddle assuming various nuclear symmetries (from Ref. 37).

FIG.3. Fission probabilities for ^{237}Np . Calculations show fit assuming an axially asymmetric first saddle point and the change when the first barrier is assumed to have an axially symmetric shape.

FIG.4. Ratio of the number of open channels available at each saddle point when different assumptions are made for the shape symmetries at the first saddle (A).

FIG.5. Fission probability data for a series of neptunium isotopes. Solid lines are fits from the microscopic statistical model described in the text (from Ref. 21).

FIG.6. Fission probability data for compound systems ^{231}Th and ^{234}Th from Ref. 26.

FIG.7. Fission probability for ^{228}Ra with model fits as described in the text (from Ref. 23).

FIG.8. Fission probabilities for plutonium, curium and californium isotopes from Ref. 25.

FIG.9. Measured fission coincidence spectra for reactions on ^{254}Es (from Ref. 36).

FIG.10. Fission probabilities and fragment anisotropies for ^{226}Ac , ^{227}Ac and ^{228}Ac (from Ref. 39).

FIG.11. Fission probability for the symmetric fission component of ^{228}Ra . Lines are model fits as described in the text (from Ref. 23).

FIG.12. Fits to resonant (t, pf) and $(, f)$ data for ^{238}U (lower portion) and to higher excitation energy $(, f)$ data. Characteristics of fits are described in the text (from Ref. 24).

FIG.13. Calculated potential energy as a function of axial $()$ and mass $(3 5)$ degrees of freedom in the vicinity of the second saddle point (from Ref. 24).

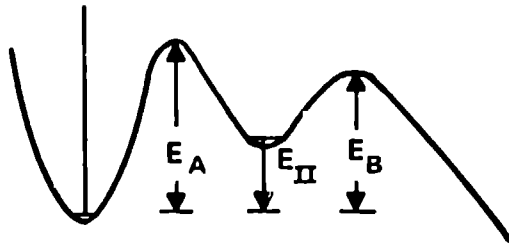
FIG.14. Fission barrier heights (E_A, E_B) from fits to experimental data. Solid points from fits to fission probability data (Ref. 37). Open points from fits to fission isomer excitation functions (Ref. 14). Solid triangles are from Ref. 44-47. Open triangles are from analyses of fission widths for sub-barrier fission resonances (Ref. 48).

FIG.15. Comparison of experimental fission barriers (Ref. 37) to various theoretical calculations from Moller 29 (solid line), Pauli and Ledergerber 30 (thin solid line) and Moller and Nix 31 (dashed lines) E_A has been corrected for effect of axial asymmetry as described in the text.

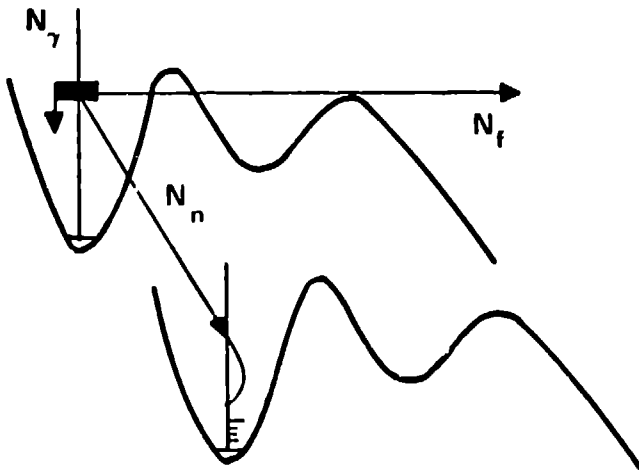
FIG.16. Evaporation residue probability for $^{236}\text{U}(^7\text{Li}, n)$ reaction from Ref. 52 .

FIG.17. Fission probability for $^{232}\text{Th}(^{12}\text{C}, ^8\text{Be})$ reaction from Ref. 52 .

NOTATION



DIRECT REACTION FISSION

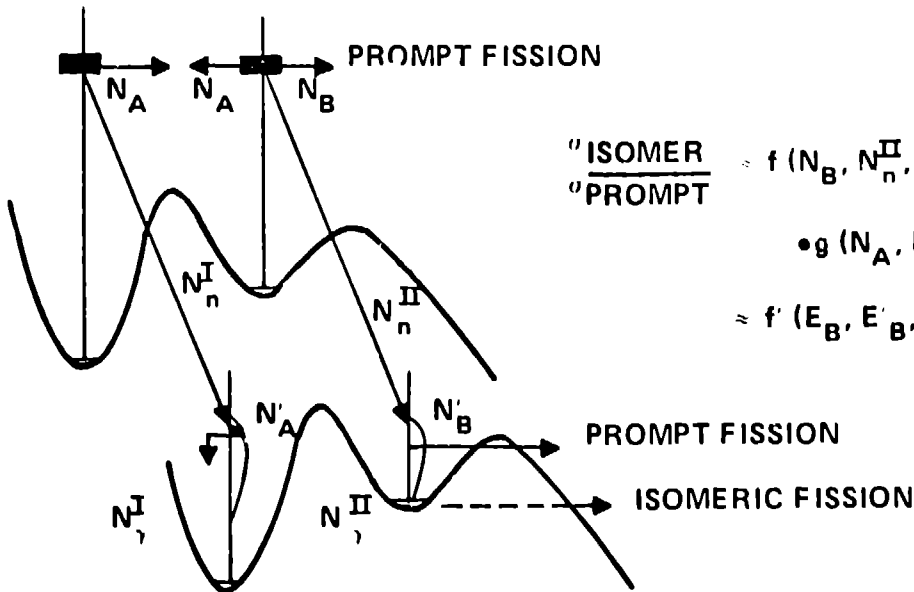


$$P_f = \left\langle \frac{N_f}{N_f + N_n + N_\gamma} \right\rangle$$

$$N = \text{EFF. NO. OPEN CHAN.} = 2\pi I/D$$

$$N_f = f(E_A, \hbar\omega_A, E_B, \hbar\omega_B)$$

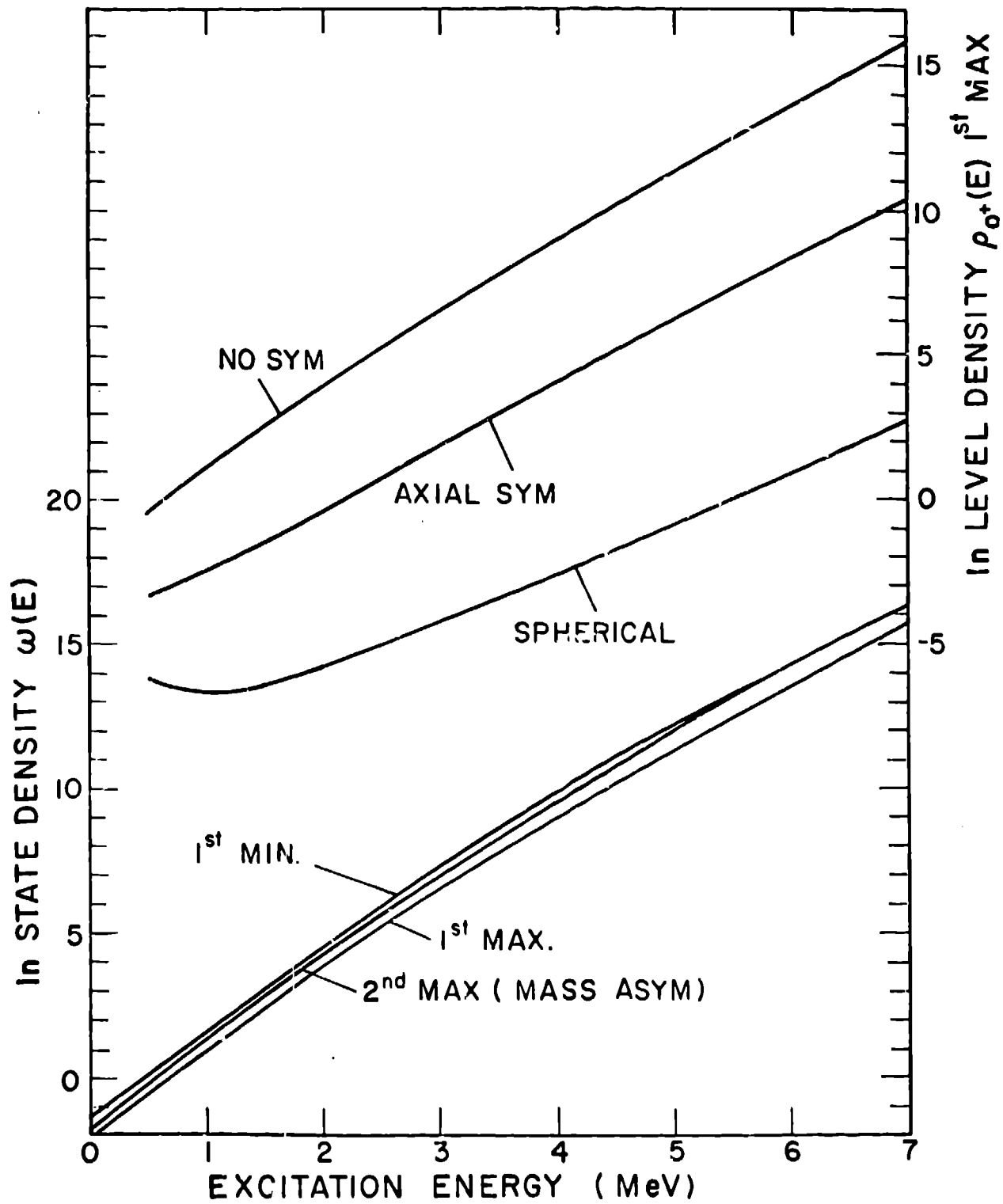
FISSION ISOMER E* FUNCTIONS

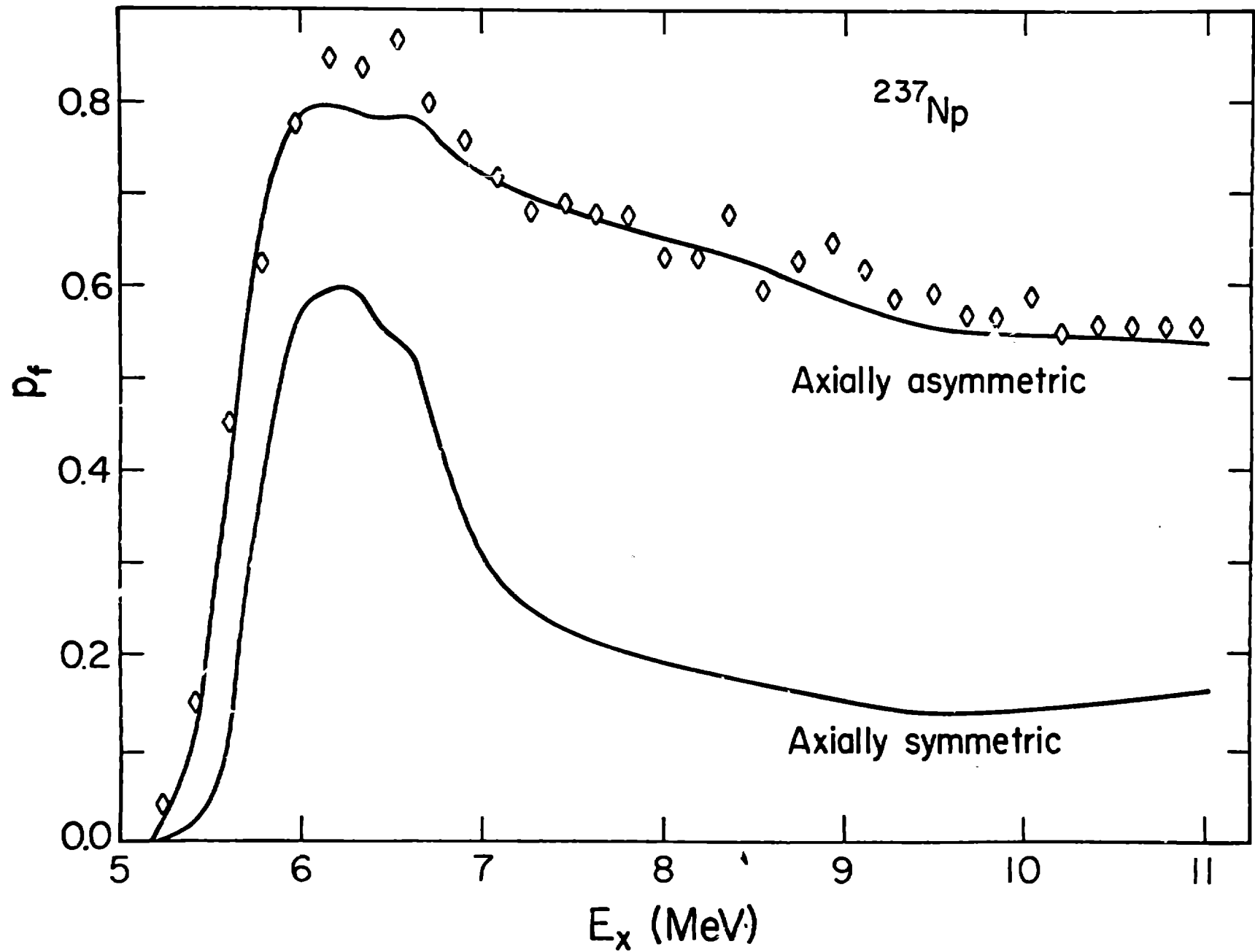


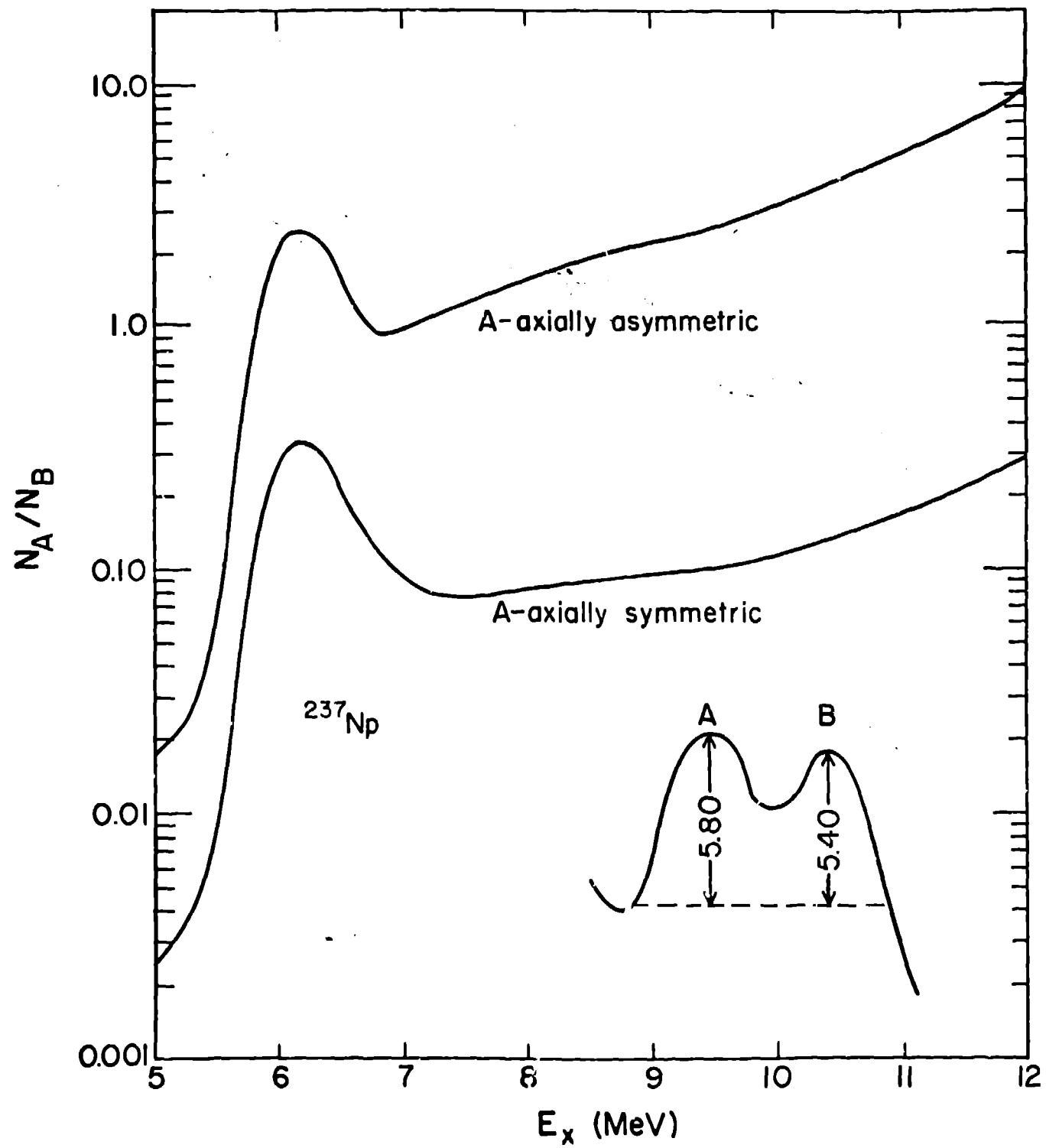
$$\frac{\text{"ISOMER}}{\text{"PROMPT}} \approx f(N_B, N_n^{II}, N'_B, N_\gamma^{II})$$

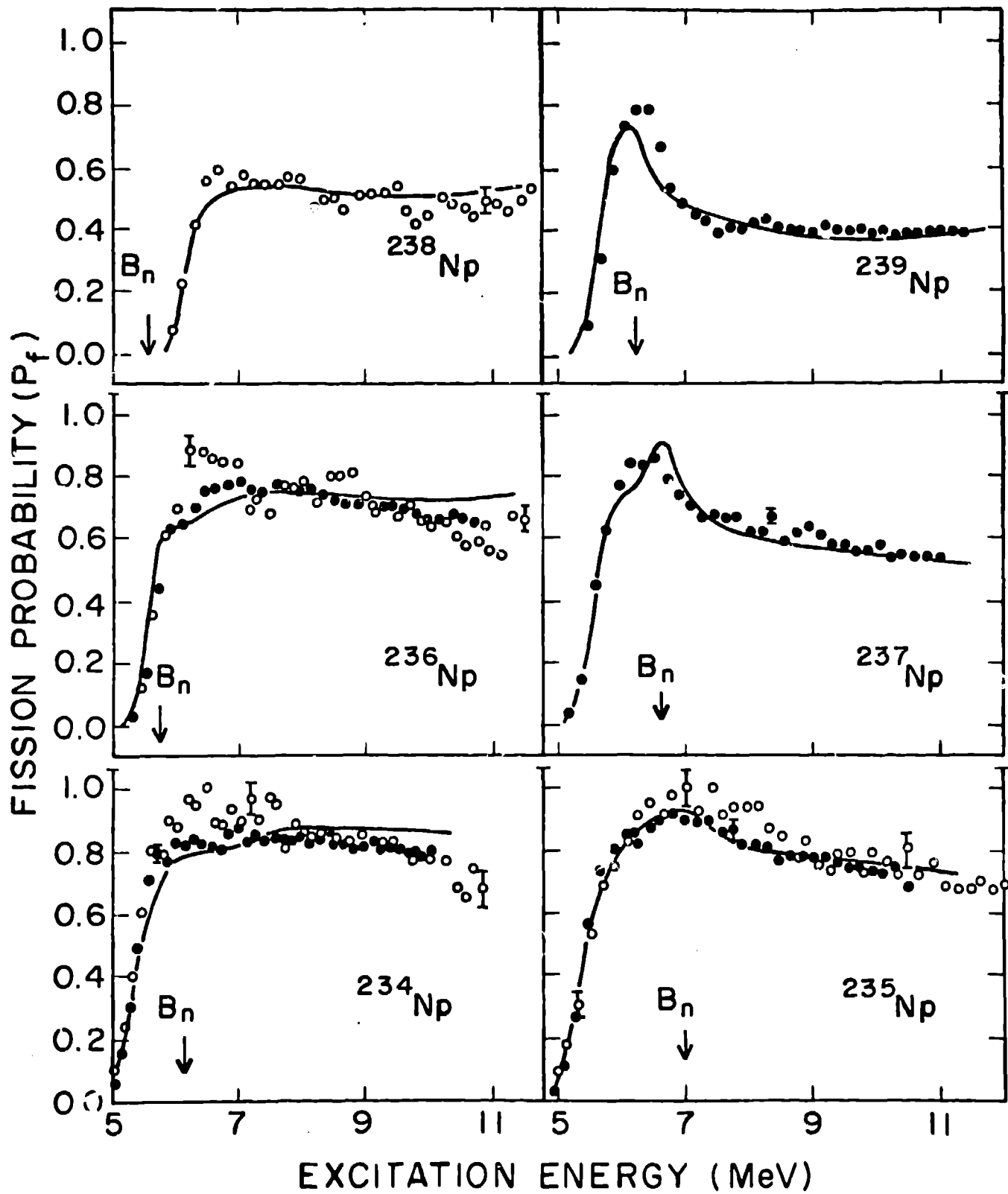
$$\bullet g(N_A, N'_A, N_n^I, N_\gamma^I)$$

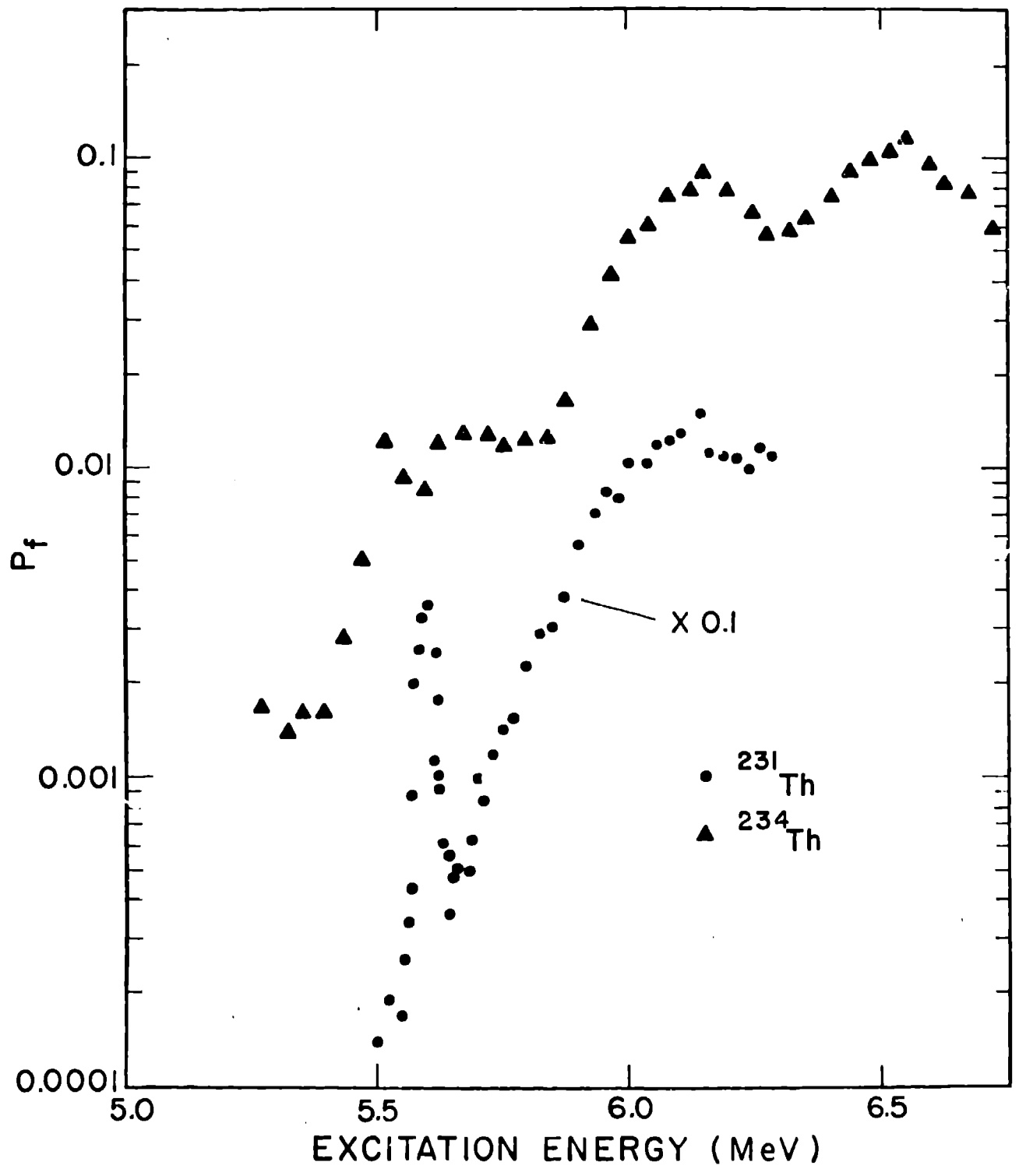
$$\approx f(E_B, E'_B, E_{II}^I) \bullet g$$

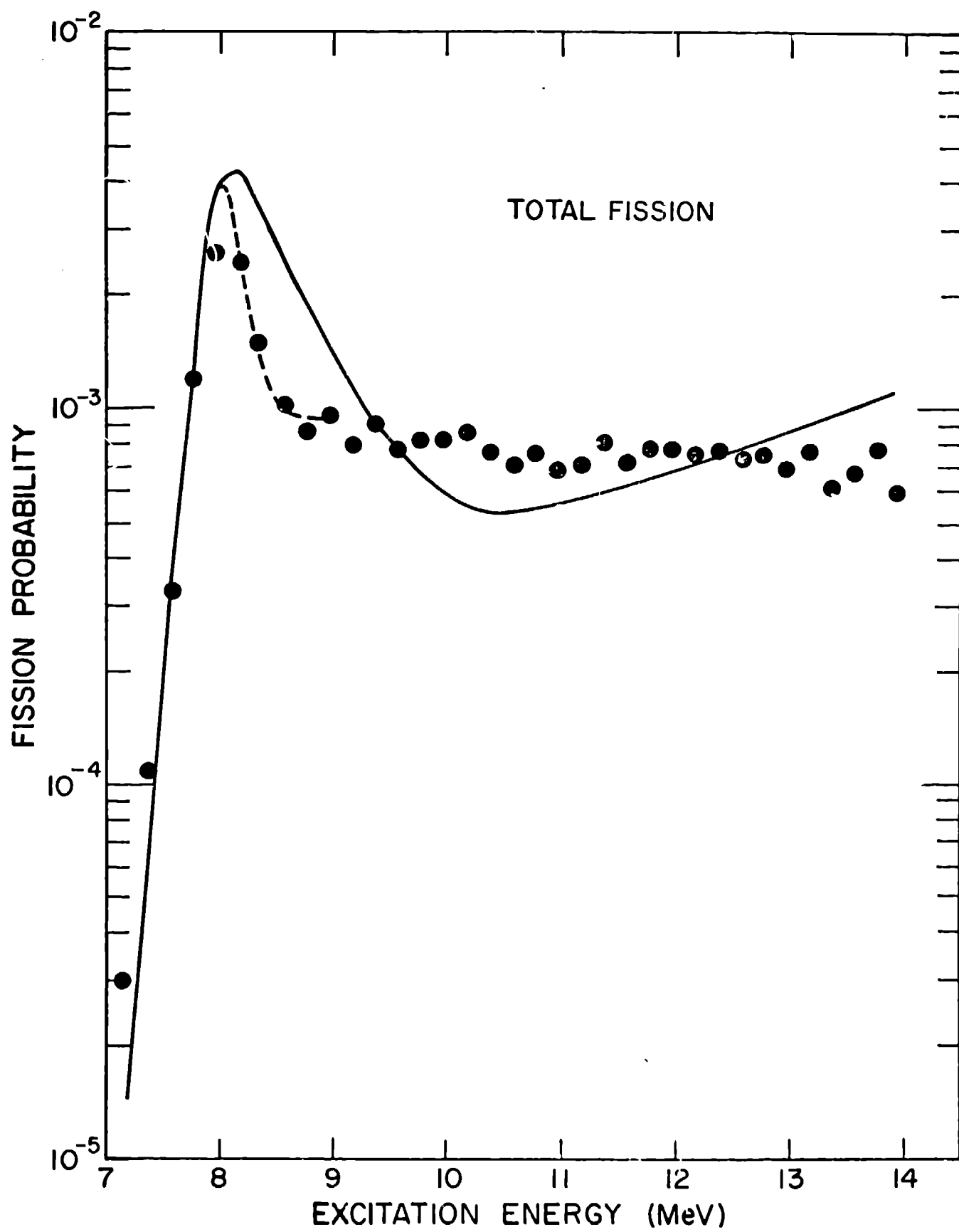


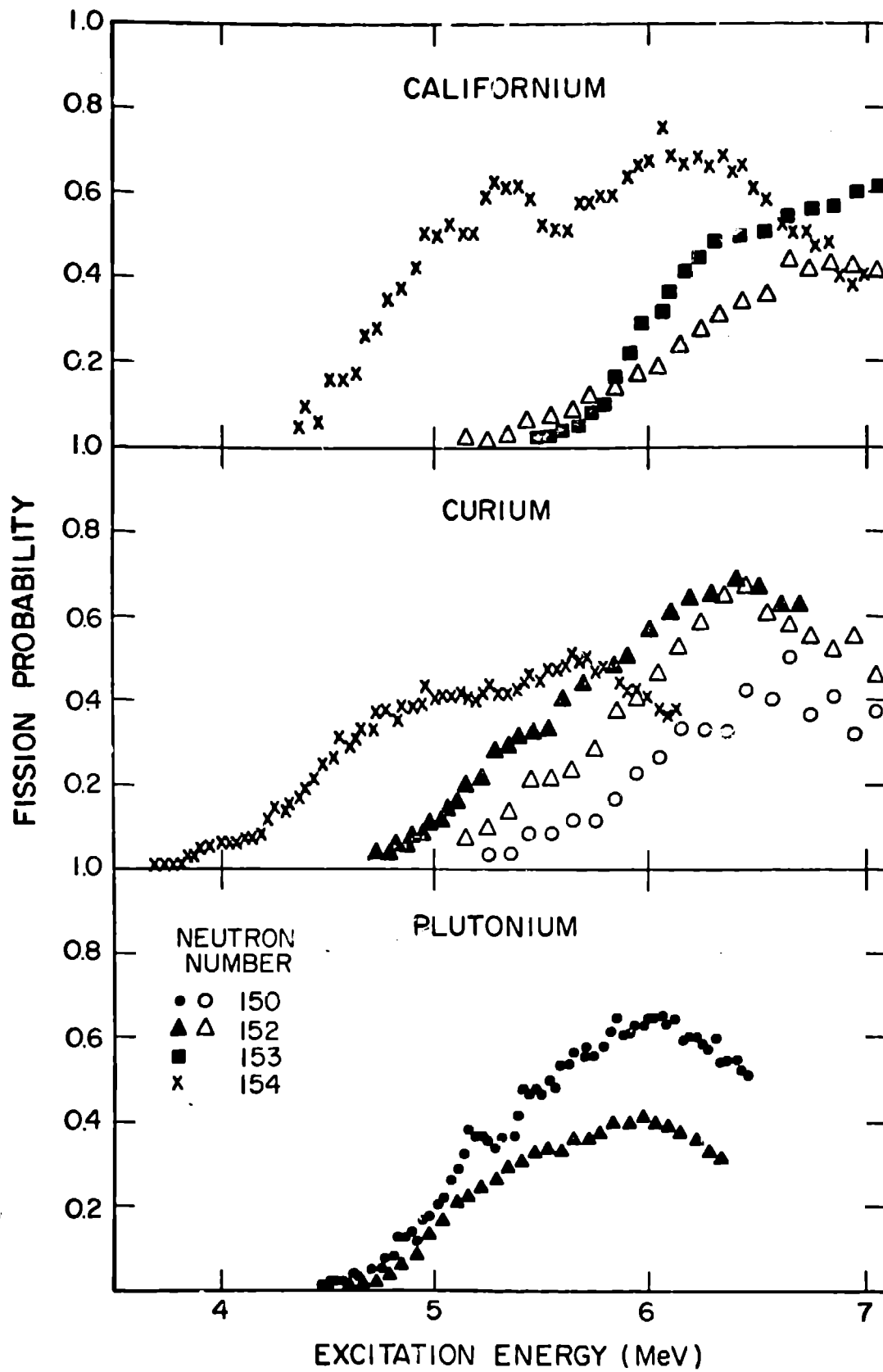


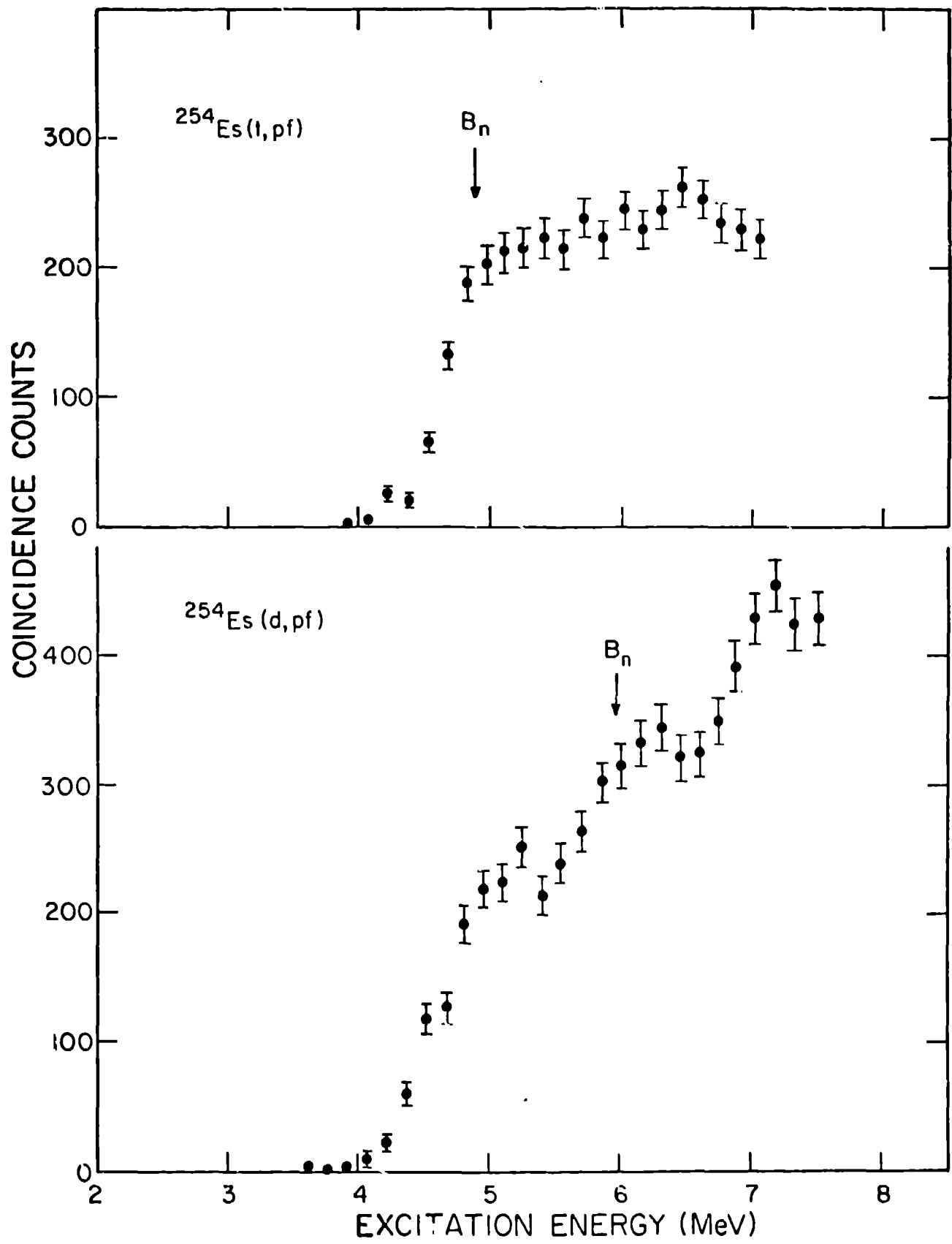




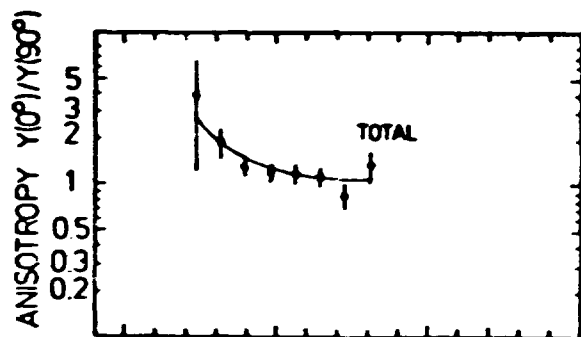




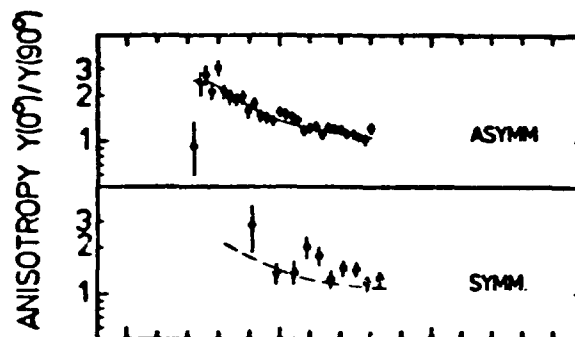




$^{226}\text{Ra}(^3\text{He,t})^{226}\text{Ac} \rightarrow f$



$^{226}\text{Ra}(^3\text{He,d})^{227}\text{Ac} \rightarrow f$



$^{226}\text{Ra}(^3\text{He,p})^{228}\text{Ac} \rightarrow f$

